Engineering Notes

ENGINEERING NOTES are short manuscripts describing new developments or important results of a preliminary nature. These Notes cannot exceed 6 manuscript pages and 3 figures; a page of text may be substituted for a figure and vice versa. After informal review by the editors, they may be published within a few months of the date of receipt. Style requirements are the same as for regular contributions (see inside back cover).

A Possible Causative Flow Mechanism for Body Rock

L. E. Ericsson*
Lockheed Missiles & Space Company, Inc.
Sunnyvale, California

Introduction

PRESENT-day high-performance aerospace vehicles are subject to unsteady flowfields which generate highly nonlinear aerodynamics with strong coupling between longitudinal and lateral degrees of freedom.[1-3] The complex vehicle dynamics are caused by separated flow effects of various types and, therefore, usually cannot be predicted by theoretical means. As a consequence, heavy reliance must be placed upon existing capabilities for dynamic testing[4] where dynamic support interference[5] and dynamic simulation problems[6] add to the difficulty of determining the full-scale, separated flow characteristics. In this Note existing experimental results for nonlinear pitch-yaw-roll coupling phenomena of high-performance aircraft are analyzed to obtain an understanding of the basic fluid mechanic phenomenon causing body rock.

Discussion

Recently, it has been demonstrated that a pointed forebody can provide a mechanism for wing rock or body rock. Wing and tail surfaces could be removed from the model of an advanced aircraft without stopping the rocking motion. Obviously, it must be the vortices shed from the pointed forebody that supply the driving mechanism for this body rock motion. The asymmetric vortex phenomenon has been studied extensively in the case of slender bodies of revolution.[7,8] It has been established that the formation of asymmetric body vortices can be dominated by the body motion,[9] and that the vortex not lifted-off moves inboard to remain very close to the surface near the centerline of the body[10,11] (Fig. 1). More recent experimental results[12] support this vortex movement (see Ref. 10 for an explanation of the experimental results[11] in Fig. 1).

Placing the cockpit in the inset sketch of Fig. 1 and considering the data by Fidler[13] (Fig. 2), one begins to see that this flow mechanism could be the cause of "body rock." It is shown in Ref. 14 that, at a critical Reynolds number, negative Magnus lift of large magnitude will be generated at very modest rotation rates on a circular cylinder. Reference 9 describes how this flow phenomenon, which is caused by moving-wall effects on boundary-layer transition,[14] can explain the results in Fig. 2. That is, the direction of even a very slow rotation determines the direction of the vortex asymmetry.

Based upon these experimental results, one obtains Fig. 3 as a possible explanation for the vortex-induced effects on the cockpit. At $t=t_1$, the body is assumed to receive the indicated rotational perturbation. The upstream moving-wall effect causes transition to move ahead of flow separation, thereby changing the separation from subcritical to supercritical, as is indicated in Fig. 3. The asymmetric vortex close to the body generates suction on the cockpit, thereby driving the rolling motion. At $t=t_2$, the cockpit has rotated to a position where it interferes with the flow separation, triggering a change from supercritical to subcritical separation. This generates a restoring rolling moment which will reverse the roll direction sometime between $t=t_2$ and t_3. At $t\leq t_3$ the roll rate is large enough to cause transition,[14] changing the flow separation from subcritical to supercritical and generating a driving rolling moment at $\phi=0$, as indicated for $t=t_3$.

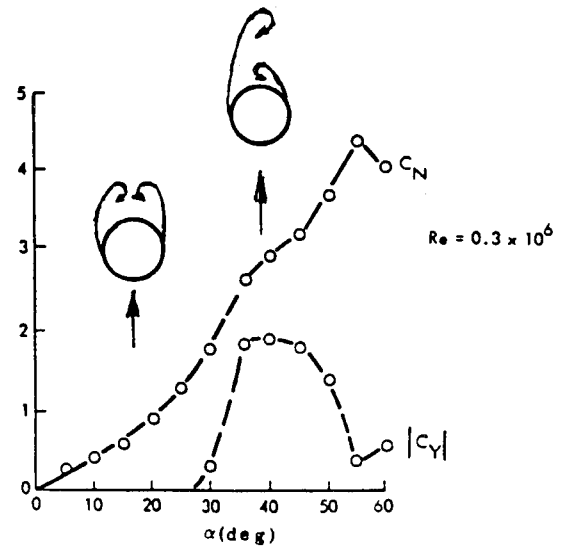

Fig. 1 Correlation of vortex-induced effects of a tangent ogive at $\beta=0$ and $Re=0.3\times10^6$ on $C_N(\alpha)$ and $C_Y(\alpha)$ (Ref. 11).

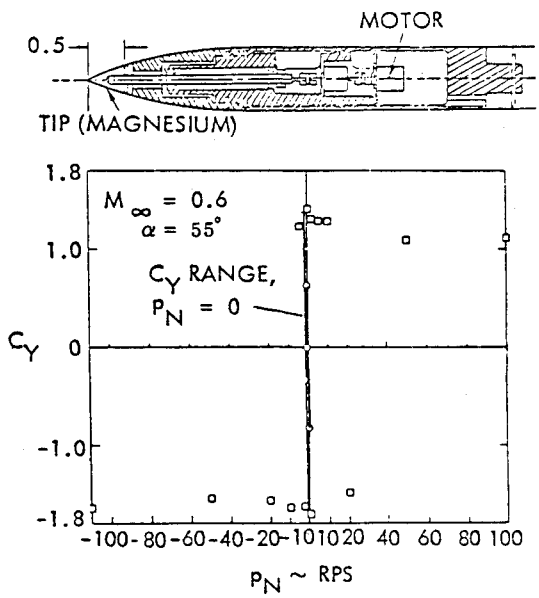

Fig. 2 Effect of spinning nose tip on vortex-induced side force at $\beta=0$ and $\alpha=55$ deg.[13]

Received Oct. 24, 1984; revision received Feb. 6, 1985. Copyright © 1985 by L. E. Ericsson. Published by the American Institute of Aeronautics and Astronautics, Inc., with permission.

*Senior Consulting Engineer. Fellow AIAA.

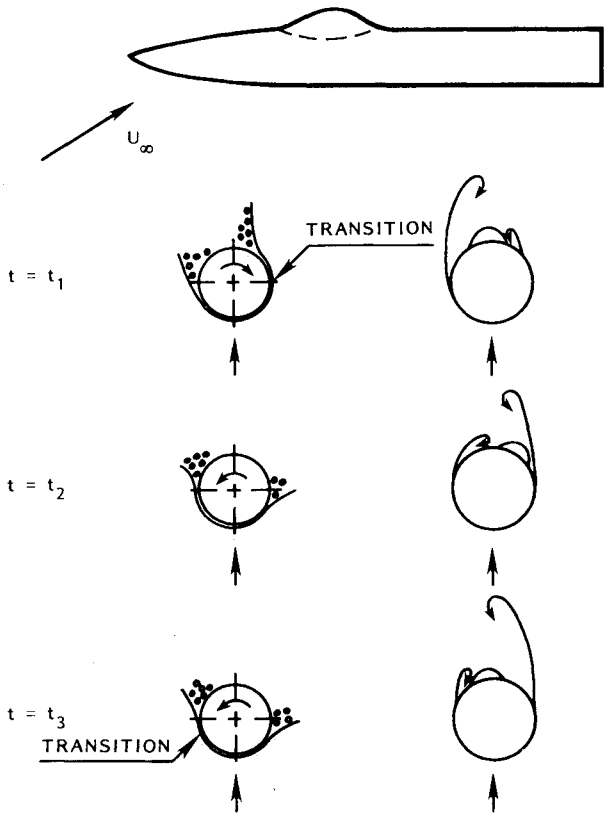

Fig. 3 Interaction between asymmetric forebody vortices and aircraft canopy.

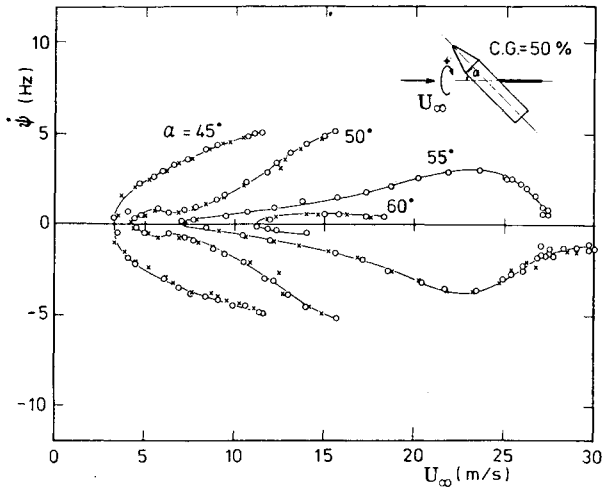

Fig. 4 Coning characteristics of cone-cylinder body at $\beta = 0$ and $\alpha \leq 60$ deg.[18]

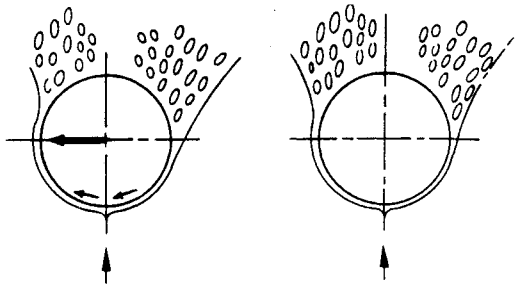

Fig. 5 Effect of coning motion on subcritical flow asymmetry.[10]

The situation is somewhat similar to that for the slender wing rock.[15,16] That is, a switch of vortex asymmetry generates the aerodynamic spring, and the associated time lag generates negative aerodynamic damping. The difference is that, in the present case of body rock, moving-wall effects add an important dynamically destabilizing flow mechanism.

The experimentally observed body rock[17] was obtained on a model that only had the roll degree of freedom (DOF). For an aircraft in free flight the asymmetry will generate the largest effect in the yaw DOF. That is, the motion will be nose-slice-dominated with relatively weak feedback from the roll DOF illustrated in Fig. 3. Recent test results[18] for a cone-cylinder, describing a coning motion at high angles of attack, illustrate the effect of nose-slice on the asymmetric vortex pair generated by a pointed slender nose (Fig. 4). The authors describe how only a slight push was needed to establish the coning motion in one direction or the other, regardless of the fact that the measured static side force was biased in one direction due to nose microasymmetries.[7,8] The body reached very nearly equal steady-state coning rates in positive and negative rotation (Fig. 4). That is, the motion dominated over the static asymmetry, locking-in the vortex asymmetry in the direction of the body motion.

A mechanism that can cause this vortex asymmetry lock-in is the moving-wall effect described earlier for the rotating cylinder.[14] The situation sketched in Fig. 5 depicts the case of a coning motion.[10] The lateral motion of the circular cross section causes the flow separation to be delayed on the advancing side and promoted on the retreating side due to moving-wall effects very similar to those discussed in Ref. 14. Thus, the motion generates a force that drives it until the equilibrium coning rate is reached (Fig. 4).

Thus, the asymmetric vortices from a slender nose at high angles of attack can drive the nose-slice motion even without any downstream interference with an aircraft canopy, or tail surfaces. With an aft fin present, a strong coupling is possible between pitch and yaw motion due to the interference effects from the nose-generated symmetric or asymmetric vortex pair, as is illustrated by experimental results.[19,20]

It should be noted that the flow mechanism for body rock exists in a limited range of α and *Re* only. Of course, the critical Reynolds number range may be relatively wide, since the transition-induced separation asymmetry can develop anywhere between the nose tip and nose shoulder on a pointed ogive or cone as the Reynolds number changes.[21]

In view of the fact that all of the nonlinear aerodynamic phenomena discussed above are generated by separated flow, one has to be greatly concerned about the applicability of subscale test data to full-scale flight conditions. Examples of the various types of simulation problems that can be encountered are given in Refs. 6, 22, and 23.

References

[1]"Dynamic Stability Parameters," AGARD CP-235, Nov. 1978.

[2]Ericsson, L. E., "Technical Evaluation Report on the Fluid Dynamics Panel Symposium on Dynamic Stability Parameters," AGARD-AR-137, April 1978.

[3]Ericsson, L. E., "A Summary of AGARD FDP Meeting on Dynamic Stability Parameters," Paper 2, AGARD CP-260, May 1979.

[4]Orlik-Rückemann, K. J., "Dynamic Stability Testing of Aircraft—Needs Versus Capabilities," *Progress in Aerospace Science*, Pergamon Press, New York, Vol. 16, No. 4, 1975, pp. 431-447.

[5]Ericsson, L. E. and Reding, J. P., "Review of Support Interference in Dynamic Tests," *AIAA Journal*, Vol. 21, Dec. 1983, pp. 1652-1666.

[6]Ericsson, L. E. and Reding, J. P., "Scaling Problems in Dynamic Tests of Aircraft-Like Configurations," Paper 25, AGARD-CP-227, Sept. 1977.

[7]Ericsson, L. E. and Reding, J. P., "Review of Vortex-Induced Asymmetric Loads—Part 1," Zeitschrift für Flugwissenschaften und Weltraumforschung, Vol. 5, Heft 3, 1981, pp. 162-174.

[8]Ericsson, L. E. and Reding, J. P., "Review of Vortex-Induced Asymmetric Loads—Part II," Zeitschrift für Flugwissenschaften und Weltraumforschung, Vol. 5, Heft 6, 1981, pp. 349-366.
[9]Ericsson, L. E. and Reding, J. P., "Steady and Unsteady Vortex-Induced Loads on Slender Vehicles," *Journal of Spacecraft and Rockets,* Vol. 18, March-April 1981, pp. 97-109.
[10]Ericsson, L. E. and Reding, J. P., "Dynamics of Forebody Flow Separation and Associated Vortices," AIAA Paper 83-2118, Aug. 1983 (to be published in *Journal of Aircraft*).
[11]Keener, E. R., Chapman, G. T., Cohen, L., and Teleghani, J., "Side Forces on Forebodies at High Angles of Attack at Mach Numbers from 0.1 to 0.7. Two Tangent Ogives, Paraboloid and Cone," NASA TMX-3438, Feb. 1977.
[12]Yanta, W. and Wardlaw, A., "Multi-Stable Vortex Patterns on Slender Circular Bodies at High Incidence," AIAA Paper 81-0006, Jan. 1981.
[13]Fidler, J. E., "Active Control of Asymmetric Vortex Effects," *Journal of Aircraft,* Vol. 18, April 1981, pp. 267-272.
[14]Ericsson, L. E., "Karman Vortex Shedding and the Effect of Body Motion," *AIAA Journal*, Vol. 18, Aug. 1980, pp. 334-344.
[15]Nguyen, L. T., Yip, L. P., and Chambers, J. R., "Self-Induced Wing Rock of Slender Delta Wings," AIAA Paper 81-1883, Aug. 1981.
[16]Ericsson, L. E., "The Fluid Mechanics of Slender Wing Rock," *Journal of Aircraft,* Vol. 21, May 1984, pp. 322-328.
[17]Chambers, J. R., Private communication of unpublished experimental results, July 16, 1982.
[18]Yoshinaga, T., Tate, A., and Inoue, K., "Coning Motion of Slender Bodies at High Angles of Attack in Low Speed Flow," AIAA Paper 81-1899, Aug. 1981.
[19]Orlik-Rückemann, K. J., Private communication of unpublished data, July 16, 1982.
[20]Orlik-Rückemann, K. J., "Aerodynamic Coupling between Lateral and Longitudinal Degrees of Freedom," *AIAA Journal*, Vol. 15, Dec. 1977, pp. 1792-1799.
[21]Keener, E. R., "Oil-Flow Separation Patterns on an Ogive Forebody," *AIAA Journal*, Vol. 21, April 1983, pp. 550-556.
[22]Ericsson, L. E. and Reding, J. P., "How to Cope with the Problems of Scaling and Support Interference in Dynamic Subscale Tests," AIAA Paper 84-0382, Jan. 1984.
[23]Ericsson, L. E., "Is the Free Flight/Wind Tunnel Equivalence Concept Valid for Unsteady Viscous Flow,?" AIAA Paper 85-0378, Jan. 1985.

A Composite Model of Aircraft Noise

Robert G. Melton*
The Pennsylvania State University
University Park, Pennsylvania

Nomenclature

$c_{1,i}, c_{2,i}$ = noise level coefficients for aircraft i
$c^*_{1,k}, c^*_{2,k}$ = composite noise level coefficients for trajectory k
i = noise source index
k = trajectory index
L^* = sound level produced by a single source delivering the same power density as N_s sources
$L_{\text{d-n}}$ = average day-night noise level
L_i = sound level from source i
L_{tot} = sound level from N_s sources
N = number of sound level samples taken in 24 h
N_s = number of sound sources
N_t = number of trajectories
r = distant (slant range) from aircraft
t = time index for sampling sound levels
w_i, w_t = time-of-day weighting factor associated with human perception of noise levels, = 1 from 7 a.m. to 7 p.m., = 10 otherwise

Received Feb. 10, 1985. Copyright © American Institute of Aeronautics and Astronautics, Inc., 1985. All rights reserved.

*Assistant Professor, Department of Aerospace Engineering. Member AIAA.

Introduction

In the analysis of aircraft noise effects on a community it has been found[1] that the separate calculation of noise levels from each aircraft contributes a significant portion of the overall computations (i.e., evaluations of noise levels and effects on the population). A method for reducing the amount of computation needed to determine these noise levels is presented. It is assumed that each aircraft can be assigned to one of several known flight paths (or that any deviations from these paths do not significantly alter the noise field on the ground).

Adding Sound Energy

The exact expression for the total sound level[2] (using any power-intensity related scale) contributed from N_s sources is

$$L_{\text{tot}} = 10 \log_{10} \sum_{i=1}^{N_s} 10^{L_i/10} \tag{1}$$

where L_i is the level produced by the ith source. Addition of the individual sound levels implicitly assumes incoherent interference of the acoustic waves, and is commonly referred to as "addition on an energy basis"; however, *power density addition* would be a more accurate characterization. Nevertheless, it provides a means for calculating the sound level from various aircraft operating in a community.

Under the assumption of isotropy in the far-field propagation of aircraft sound, the approximation for the level at distance r from the ith source is

$$L_i = c_{1,i} - c_{2,i} \log_{10} r \tag{2}$$

Using data obtained from the Integrated Noise Model,[3] values of c_1 and c_2 were calculated from least-square-error fits, and the results are shown in Table 1. A plot of sound level (in this case, the A-weighted level, L_A) vs r for Boeing 737-100/200 aircraft appears in Fig. 1.

The concept of "energy addition" is also employed in various other measures of noise, notably those that include some weighting of the incident power based upon the time of day and the resulting human perception of the sound level. For example, the average day-night level $L_{\text{d-n}}$ is defined as

$$L_{\text{d-n}} = 10 \log_{10} \sum_{t=1}^{N_t} w_t 10^{L_{A,t}/10} / N_t \tag{3}$$

Clearly, $L_{\text{d-n}}$ is based upon a weighted *average over time* of the incident power. The order of occurrence of the various sound level contributions is irrelevant, as long as the appropriate weighting is assigned to each.

This concept raises the possibility, for simulation purposes, of replacing a number of aircraft moving along a specified trajectory with a single "equivalent source" that delivers the same weighted average power distribution to points on the ground.

Composite Model

Using Eqs. (1) and (2), and continuing to use $L_{\text{d-n}}$ as the prototype, the equivalent level at distance r from all sources on the kth trajectory is

$$L^*_k(r) = 10 \log_{10} \sum_{i=1}^{N_s} w_i 10^{L_i(r)/10} \tag{4}$$